

# **ATMOSPHERIC CONSEQUENCES OF COSMIC RAY VARIABILITY IN THE EXTRAGALACTIC SHOCK MODEL**

Adrian L. Melott<sup>1</sup>, Alex J. Krejci<sup>1</sup>, Brian C. Thomas<sup>2</sup>, Mikhail V. Medvedev<sup>1</sup>, Graham W. Wilson<sup>1</sup>, and Michael J. Murray<sup>1</sup>

## **ABSTRACT**

It has been suggested that galactic shock asymmetry induced by our galaxy's infall toward the Virgo Cluster may be a source of periodicity in cosmic ray exposure as the solar system oscillates normal to the galactic plane, thereby inducing an observed terrestrial periodicity in biodiversity. There are a number of plausible mechanisms by which cosmic rays might affect terrestrial biodiversity. Here we investigate one of these mechanisms, the consequent ionization and dissociation in the atmosphere, resulting in changes in atmospheric chemistry which culminate in the depletion of ozone and a resulting increase in the dangerous solar UVB flux on the ground. We estimate the enhancement of cosmic ray intensity for a range of reasonable parameters of the galactic wind and galactic magnetic field, and use these to compute steady-state atmospheric effects. At the lower end of this range, we find that the effects are far too small to be of serious consequence. At the upper end of this range, the level of ozone depletion approaches that currently experienced due to anthropogenic effects such as accumulated chlorofluorocarbons, i.e. ~2.1 % global average loss of ozone column density. We discuss some of the possible effects. While much smaller intensity than atmospheric effects of a nearby galactic gamma-ray burst, the duration of the effects would be about  $10^6$  times greater. Current

ozone depletion is a documented stress on the biosphere; it is not clear whether its consequences would be severe if of extended duration. We conclude that for estimates at the upper end of the reasonable range of the cosmic ray variability over geologic time, the mechanism of atmospheric ozone depletion may provide a small additional stress, enhancing the impact of other events. However, in order to account for large fluctuations in biodiversity correlated with cosmic ray flux, other mechanisms should be investigated.

<sup>1</sup> University of Kansas, Department of Physics and Astronomy, 1251 Wescoe Dr. # 1082, Lawrence, KS 66045-7582; [melott@ku.edu](mailto:melott@ku.edu), [akrejci@gmail.com](mailto:akrejci@gmail.com), [medvedev@ku.edu](mailto:medvedev@ku.edu), [gwwilson@ku.edu](mailto:gwwilson@ku.edu), [mjmurray@ku.edu](mailto:mjmurray@ku.edu)

<sup>2</sup> Washburn University, Department of Physics and Astronomy, Topeka, KS 66621; [brian.thomas@washburn.edu](mailto:brian.thomas@washburn.edu)

## 1. Introduction

A  $62 \pm 3$  My periodicity in fossil biodiversity that goes back more than 500 My has been found in one paleontological database at better than 99% confidence [Rohde and Muller 2005, hereafter RM; Cornette 2007; Lieberman and Melott 2007]. More recently, it has been found in an independent database controlled for systematic error [Melott 2008]. Medvedev and Melott [2007; hereafter MM] proposed a mechanism for this periodicity based on the motion of the Sun normal to the galactic plane. Although there is considerable uncertainty in the global mass density of the galaxy, the motion is quasiperiodic (due to nonuniformities) at about 63.6 My, equal within uncertainties to that of the biodiversity periodicity, and in phase with it [Gies and Helsel 2005; Binney 2006]. Departures from axial symmetry due to spiral arms introduce scatter in such solutions of only a few My over the last 500 My, as shown by Svensmark [2006]. This is comparable to the size of the bandwidth in the RM fit to the principal periodicity. Thus, any effect lowering biodiversity upon excursion to Galactic north would have the right sense.

MM proposed that there are heightened cosmic rays (CR) of energies  $\sim$ TeV and above from a galactic termination shock and possibly a bow shock as well, associated with the Galaxy's well-known infall toward the Virgo Cluster. The solar system is shielded from these cosmic rays when inside or south of the galactic disk by the turbulent magnetic field of the galaxy, but there is substantially increased exposure at galactic north. In distinction to sources such as gamma-ray bursts or solar flares studied in our previous work on astrophysical ionizing radiation effects, this excess irradiation would persist for  $\sim 10^7$  y of each cycle.

One fairly obvious possibility for impact on biodiversity is direct effects of radiation. Although most of the energy of cosmic rays is deposited in the atmosphere, some reaches the ground particularly in the form of muons ( $\mu$ ) which comprises about 85% of the equivalent biological dose of CR in the USA; in turn CR products constitute about one-third of the annual dose in the USA [Alpen 1998]. Increased exposure with altitude is the presumed cause of increased cancer rates among airline personnel [e.g. Pukkala et al. 1995]. Cancer rates correlate strongly with cosmogenic  $^{10}\text{Be}$  [primarily formed in CR interactions with the atmosphere] as well as with latitude, in an apparent effect on the germ cells of one's parents [Juckett 2007]. Low-energy cosmic ray dose increases toward the poles, due to guiding effects of the Earth's magnetic field. Study of bone cancer in dinosaur fossils shows no evidence for a radiation effect [Natarajan et al. 2007], but the K-T extinction (known to most of us as the dinosaur event) is apparently out of phase and not part of the 62 My periodicity (MM).

An additional class of effects is connected to changes in atmospheric chemistry. The triple bond of  $\text{N}_2$ , which comprises about 80% of the atmosphere, is very strong. Organisms have devised a number of strategies for breaking this bond locally so that nitrogen can become chemically available. CRs or high-energy photons are able to break this bond high in the atmosphere, which leads to formation of a number of compounds which are normally only present at low abundance. This includes NO and  $\text{NO}_2$ , which are referred to as  $\text{NO}_x$ . These compounds persist in the atmosphere for years, being slowly removed primarily by rain or snow precipitation as nitric acid [ $\text{HNO}_3$ ], as well as by photolysis. For details see Thomas et al. [2005].

There are two main overt chemical effects of potential importance. (1) The most important

effect of  $\text{NO}_x$  appears to be ozone ( $\text{O}_3$ ) depletion [Ruderman 1974; Ejzak et al. 2007, and references therein].  $\text{NO}_x$  catalyze the conversion of  $\text{O}_3$  to ordinary oxygen molecules. Stratospheric  $\text{O}_3$  absorbs strongly in the UVB (280-315 nm) band, removing about 90% of it. UVB is strongly absorbed by and damages DNA and proteins, and is a known carcinogen and mutagen. Nearby supernovae and galactic gamma-ray bursts are candidates for catastrophic ozone depletion. (2) Secondly, the brown gas  $\text{NO}_2$  may have some effects of opacity [Melott et al. 2005]. This effect is subdominant to ozone depletion, and is only likely to be serious in extreme cases. We have examined the opacity as described in the next section. We also expect some production of  $\text{NO}_x$  and (ironically)  $\text{O}_3$  in the troposphere. These compounds are toxic. This is not an issue in previous studies based on ionizing photons, but the cross sections are such that we may expect energy deposition lower in the atmosphere. We have studied these two effects and report our (largely negative) conclusions in this paper.

There is a large literature on the association of low-altitude cloud formation with cosmic rays; for a review see Scherer et al. [2007]. Clouds may increase albedo, lowering the global temperature. The most robust conclusion seems to be that that CR flux probably forces climate on long timescales, but that recent warming cannot be attributed to reduced cosmic ray flux [Lockwood and Fröhlich 2007]. The CRs on which past studies were based are low energy, modulated by the Earth's magnetic field and the solar wind. TeV CRs would not be so modulated. Furthermore, their energy deposition lower in the atmosphere might be even more conducive to low-level cloud nucleation. Lower temperatures from increased albedo, if present, would be expected to lower biodiversity [Aguirre and Riding 2005, and references therein].

The purpose of this study is to model the potential atmospheric chemical effects of the increased CR flux associated with the MM hypothesis, and estimate the magnitude of potential biological or climatic consequences based on NO<sub>x</sub> production and O<sub>3</sub> depletion. Direct radiation effects on organisms and possible cloud nucleation mechanisms are not included in this study.

## 2. Methods

The hypothesis of enhanced cosmic ray flux correlated with excursions of the Sun to Galactic north assumes that there will be substantially lower shielding from the galactic magnetic field at those times. The enhanced flux originates in CRs accelerated at shocks which are closer to the Galaxy on the north side, toward the Virgo Cluster (MM). Only rough estimates are available of the magnitude and functional shape of the enhanced spectrum. We will parameterize the CR flux spectrum as a function of CR energy  $E$  and our displacement  $z$  from the galactic plane. This parameterization is based on the model described in MM, where the slope beyond the knee (-3.2) is assumed to be the “true” flux in the neighborhood of our Galaxy, suppressed by the magnetic field inside the disc.

$$F(z,E)= C_n \{E_p^{-2.7} \exp[-(E_p/3)^{0.5}] + f(z) E_p^{-3.2} \exp(-E_0/E_p)\} \quad [1]$$

Where  $C_n$  is a normalization constant,  $E_p$  is the energy in PeV,  $E_0$  is a variable cutoff in the same units, and  $f(z)$  parameterizes the enhancement due to solar position. The first term represents the normal, lower-energy contribution by sources inside the galaxy [presumably largely supernova remnants]. When  $E_0 = 3$  PeV,  $f(z)=1$ , the CR spectrum observed locally, where  $z$  is small (~8 pc)

is reproduced [to within the accuracy we need], and the contributions approximately meet at the knee. This functional form is not particularly valid for  $E > 3$  or for  $f(z) < 1$ ; this does not concern us because contributions from energies above the knee are negligible, even in the enhanced state, and we will not consider the suppressed state, ie when  $z < 0$ . Estimates of the range of enhancement consistent with extragalactic backgrounds, pressure, etc. lead us to study 2 cases here:  $E_0 = 10^{-3}$  in case 1, and  $10^{-4}$  in case 2; and  $f(z)$  adjusted so that the subsequent flux at 1 TeV is enhanced by a factor of 4 (case 1) or 25 (case 2). Case 1 is an estimate based on the best estimates of relevant parameters, and Case 2 the maximal value consistent with existing constraints (MM). While far from exhaustive, this will enable us to do a preliminary exploration of parameter space in order to determine whether interestingly large atmospheric effects are possible and worthy of more detailed exploration in the future. In Figure 1 we show the range of CR spectra we investigate in our model, including the unperturbed case. We do not include the present lower-energy background in these figures, because its energy deposition is built into the atmospheric code (described below).

Deleted:

We performed our modeling using the Goddard Space Flight Center two-dimensional (latitude, altitude) time-dependent atmospheric model that has been used extensively to study the effects of solar flares, as well as supernovae and gamma-ray burst effects. We will describe the code only briefly, given accounts elsewhere [see Thomas et al., 2005; Ejzak et al., 2007; Thomas et al., 2007; and references therein]. There are 18 bands of latitude and 58 log pressure bands. The model computes atmospheric constituents in a largely empirical background of solar radiation variations, with photodissociation, and including winds and small scale mixing. It also includes an empirical background of CR source ionization, which includes an 11-year solar modulation

cycle, all with a timestep of one day.

Our CRs are of much larger primary energy than normal galactic CR, so we cannot simply turn up the usual background, as was reasonable in supernova studies [Gehrels *et al.* 2003]. CRs of energy  $10^{11}$  eV and up are likely to form the enhanced population; they will not be particularly affected by the solar wind or geomagnetic field, and due to smaller cross sections will deposit energy lower in the atmosphere. To simulate the air showers we used CORSIKA [e.g. Djemil *et al.* 2005; see <http://www-ik.fzk.de/corsika/>], a program for detailed simulation of extensive air showers initiated by high energy cosmic ray particles. Our procedure and the openly available table of our results is described elsewhere in more detail [Krejci *et al.* 2008]; we summarize it here briefly. We have done 25 simulated showers at each of a series of energies separated by 0.1 in  $\log_{10}$  of primary energy between 10 GeV and 1 PeV, i.e. at 50 different primary energies. We use this energy deposition information convolved with our assumed spectra of enhanced CR, considerably extending the range of the NGSFC code and making possible the treatment of energetic particles of arbitrary energy up to PeV as a source of atmospheric ionization.

It is computationally unfeasible at this time to do Monte Carlo over all possible angles of incidence, so we investigated and applied an approximation scheme. We investigated the effect of zenith angle by doing 25 shower ensembles (1250 simulation runs) each at zenith angles of  $0^\circ$  (vertical),  $45^\circ$ , and  $70^\circ$ , over the range of energies noted above, weighted by  $E^{-2.7}$  as in the normal CR spectrum. In Figure 2a we show the fractional energy deposition for each of these zenith angles (excluding nuclear interactions) per interval in log pressure, proportional to total column density traversed by the shower, which is approximately linear in altitude. Note that the



lateral displacement in the lines, and the location of their maxima, are reasonably approximated by a  $(\cos \theta)^{-1}$  factor, the simplest thing one would expect from a column density factor. At the level of approximation needed for this assessment of the atmospheric ionization, we should replace the ensembles of angles of incidence by a single ensemble at  $\text{arc cos} \langle \sin \theta \cos \theta \rangle$ , where the mean  $\langle \rangle$  is over a hemisphere; this is  $\text{arc cos} (\pi^{-1})$ , or  $71.44^\circ$ . At the level of precision needed for this study, and given the complications in using CORSIKA for greater incidence angles, we have used the  $70^\circ$  ensemble for this purpose. Since in the MM hypothesis the solar system resides in a region of excess CR flux for of order  $10^7$  y, we take this angle-averaged flux for all points on the globe. Given the assumed flux levels, the atmosphere reaches a steady-state in about 10 years. Our results will be presented in the steady-state approximation, long after the flux is “turned on”, but will still show seasonal and solar cycle fluctuations.

For each shower, we recorded the fractional energy deposition in each of 1000 bins of  $1 \text{ g/cm}^2$  column density. The dispersion in these quantities between showers of the same primary energy is not great. We used their mean to construct a lookup table describing the energy deposition for a given primary energy as a function of pressure. We then used this lookup table to construct the total energy deposition of a given spectrum of CR primaries.

The greatest deposition of energy per bin is in the first or second bin, corresponding to a first interaction very high in the atmosphere. Since log column density is nearly linear with altitude, we plot energy deposition per log column density. In Figure 2b we show for our lowest and highest energy primaries, at a  $70^\circ$  incidence angle. This has a weak trend with primary energy, corresponding to deeper penetration into the atmosphere for higher primary energies, due to

somewhat lower interaction cross sections.

This gives (for  $70^\circ$  zenith angle) about  $60 \text{ g/cm}^2$  as the site of the greatest deposition of energy per unit distance, corresponding to an altitude of about 20 km. This can be compared with (a) about 13 km as the altitude of maximal energy deposition density for the normal CR spectrum as implemented in the NGSFC code, strongly biased toward high latitudes, and (b) 22 to 35 km as the peak deposition for keV-MeV photons, depending upon energy [Ejzak et al. 2007]. Recall that ozone ( $\text{O}_3$ ) depletion is the primary effect of interest here.  $\text{O}_3$  lives at altitudes of 10-35 km [e.g. Harfoot et al. 2007], with considerable latitude dependence [Ejzak et al. 2007]. The results we will present are partially a result of these differing altitude distributions. The apparent discrepancy between the altitudes in (a) and (b) and the difference in cross sections results from the fact that the normal dominant CR spectrum up about a GeV, is strongly guided by the Earth's magnetic field, comes down with a small zenith angle near the poles, and consequently encounters a lower mean column density than an isotropic ensemble.

Deleted: (

### 3. Results

Our primary result is that the changes in atmospheric chemistry are considerably different for our two cases of the EGCR enhancement. We report here two ways of viewing effects on  $\text{O}_3$  due to the enhancements: 1) changes in globally averaged  $\text{O}_3$  column density and 2) changes in profile  $\text{O}_3$  volume number density. Both are reported as percent differences, comparing point-wise between a run with the EGCR enhancement and a run with only the normal background. From the point of view of ground-level UV, column density is the most important result. We

turn on the cosmic ray flux in a background model of the present atmosphere, and run until the transients have been effectively removed, which takes more than a decade. After this point there is no long-term accumulation of NO<sub>x</sub>. Column density changes are shown in Figures 3a and 3b over 200 months, representative of the steady state. Variations here are due to seasonal and solar cycle changes which affect photolysis reactions that are important for O<sub>3</sub>. Depletions for case 1 (Figure 3a) range around -0.03%. These are small compared with changes that took place over longer timescales due to changes in atmospheric oxygen concentration and solar luminosity [Björn and McKenzie 2007; Harfoot et al. 2007]. Furthermore, they are small compared with the level change necessary to induce serious damage to the biosphere (e.g. Jagger 1985; Häder et al. 2003). We conclude that changes in case 1 are too small to have a major effect on the biosphere, even with assumed 10<sup>7</sup> year durations.

For case 2 (Figure 3b), column density changes are more significant, ranging around -2.1%. This is only slightly less than present ozone depletion due to anthropogenic sources. Earth's orbital resonances will cause larger and more rapid variations in the O<sub>3</sub> column density at specific seasons, but not in the mean annual column density [Björn and McKenzie 2007; Shaffer and Cerveny 2004]. There are a variety of geological and biological proxies being developed to monitor past O<sub>3</sub> layer levels, but all are in developmental stages at this time. We will present only a summary of the results, arguing that greater detail is not justified in this case. Case 2 appears to be a possible additional stressor to the biosphere, but it is apparently very far from the level needed for mass extinctions, and can only be considered viable as an additional source of stress acting in concert with other kinds of events, when continuing for many My.

Column density changes are the net result of both production and depletion of ozone throughout the altitude profile. Figures 4a and 4b show point-wise changes in profile  $O_3$  volume number density at month 252, which corresponds to March and represents a middle value in column density changes for both cases. As seen above, changes are significantly greater for case 2. However, both cases show qualitatively similar effects in profile changes. A border exists between depletion of  $O_3$  at higher altitudes and production of  $O_3$  at lower altitudes. This border runs from about 15 km at the North Pole to about 30 km at the Equator to about 20 km at the South Pole. Production at lower altitudes occurs for two primary reasons: 1) Depletion of  $O_3$  by  $NO_x$  at higher altitudes allows solar UV to penetrate deeper into the atmosphere than normal, which dissociates  $O_2$  molecules leading to production of  $O_3$ . 2) At lower altitudes,  $NO_x$  compounds produced by cosmic rays can be photolyzed to produce O which then reacts with  $O_2$  to produce  $O_3$ . We note that production values here are somewhat misleading, appearing relatively large because  $O_3$  number densities are normally small at lower altitudes. Figure 5 shows the normal  $O_3$  number density profile for this month. We note that in case 2, ground level  $O_3$  is increased by only about 1-4 % which is not a large enough increase to be toxic.

In comparison to our previous studies involving photon events [Ejzak *et al.* 2007, Thomas *et al.* 2005], we see larger production of  $O_3$  at low altitudes in the present cases. This is primarily a difference in where energy is deposited in the atmosphere. The photon events typically had a peak energy deposition around 35 km while in these cases the energy deposition peaks at about 20 km. More  $NO_x$  is therefore produced at lower altitudes where  $O_3$  is normally sparse and hence photochemical production is more efficient.

Our examination of opacity is motivated by the possibility that climate might be cooled by reduced transmission of solar energy to the surface. We find that with the maximal case 2, only a global average of about 0.07% of solar energy, or a maximum of 0.1% near the poles, is absorbed by NO<sub>2</sub>; of course it is much less in case 1. Based on previous studies [Solanki and Krivova 2003; Foukal et al. 2006], we estimate that this would induce a cooling of only about 0.1 °C in the maximal case 2, and is therefore unlikely to have a major effect on biodiversity.

#### **4. Discussion**

We have employed a widely-used cosmic ray air shower code to model the energy deposition of cosmic ray primaries in the range 0.1-1000 Tev. We have convolved the resulting distribution function with the spectrum of two cosmic ray energy spectra. The first one is based on the most likely parameters while the 2<sup>nd</sup> has the maximum increase in CR flux consistent with current uncertainties in describing intergalactic shocks. The resulting energy deposition extends the useful energy range of the NASA-Goddard Space Flight Center 2D atmospheric code, to model the response of the atmosphere to the enhanced EGCR flux hypothesized by MM. In doing so, we have performed a first-order evaluation of the plausibility of one of the mechanisms of stress on the biosphere which might result from the enhanced CR flux. We have found that in case 1 the magnitude of the stratospheric O<sub>3</sub> depletion as well as tropospheric O<sub>3</sub> synthesis is so small that the primary effect examined here, enhanced solar UVB is very small. In case 2, the effect is greater, with a globally averaged fractional depletion of about 2.1% in O<sub>3</sub> with localized maxima about 5 times larger.

The reduced O<sub>3</sub> allows more UVB, 280-315 nm to reach the surface. The levels we find in the case 2 simulation are comparable to those noted from current anthropogenic O<sub>3</sub> depletion, reaching a global average of order 3%, where it may have stabilized since the banning of chlorofluorocarbon refrigeration and propellant compounds. The current situation may be used as a kind of template to characterize the effects that might result from enhanced UVB.

UVB has a wide variety of damaging effects on organisms. These include a number of different kinds of damage to DNA; inhibition of growth in seedlings and inhibition of the synthesis of essential organic compounds; photocarcinogenesis and skin edema in animals; damage to the cornea, inhibition of motility in microorganisms [Madronich 1993]. Terrestrial plants show a variety of effects, including reduced growth rates and enhanced sensitivity to pollutants and elevated temperature [Tevini 1993]. Effects on aquatic ecosystems are severe, affecting motility of organisms and photosynthetic efficiency. There are indications that UVB reduces photosynthesis in Antarctic waters by as much as 25% with current levels of ozone depletion. As much as 20% of the current global primary food production is in the southern oceans [Häder 2003]. Field experiments on amphibians [Blaustein *et al.* 1998] show that the hatching success of eggs may be strongly affected, at all altitudes. A meta-analysis of UVB effects [Bancroft *et al.* 2007] found an overall negative effect on both survival and growth across life histories, trophic groups, habitats, and experimental venues. Despite the overall negative effect, there were large variations of intensity: for example, embryos were affected quite strongly. Contrary to the experimental hypothesis, there were no systematic differences (for example between fresh water and marine habitats, or with altitude. UVB was found to interact synergistically with other stressors such as contaminants, disease, and extreme thermal events. In fact, UVB acts in a

strongly synergistic way with nitrate [*Hatch and Blaustein 2000*], and nitrate would also be enhanced as the NO<sub>x</sub> are rained out of the atmosphere [*Melott et al. 2005*]. This, combined with diffusion down from the stratosphere, is the primary removal mechanism after the initial transient bout of photolysis. Elsewhere [*Thomas and Honeyman 2008*], we have examined whether the nitrate deposition following a large ionization event (a 100 kJ m<sup>-2</sup> GRB) would be great enough to cause enhanced amphibian damage, in combination with elevated UVB levels. We have found that the increase in nitrate concentrations would not be significant in that case. Given that the present study involves much smaller atmospheric effects it is unlikely that nitrate deposition would have any effect here.

UVB effects strongly contribute to amphibian decline [*Kiesecker et al. 2001*] which is proceeding at over 200 times the background rate [*McCallum 2007*]. Major effects are being seen in plankton, with the present UVB increase [*Davidson 1998*]. On the other hand, one cannot discount the possibility of an evolutionary adaptation to the increased UVB levels, and UVB cannot be shown to be the sole cause of these declines.

We recall that while atmospheric effects in Case 1 are clearly too small to be significant, those in Case 2 are comparable present-day O<sub>3</sub> depletion, which is widely acknowledged to be a crisis at least for oceanic surface life and amphibians. It is possible that Case 2, which was constructed as a strongest-case scenario, if the steady state were continued for ~10<sup>7</sup> years as indicated by the orbital motion of the Sun in the Galaxy, might show large effects on biodiversity, by providing an additional stress. However, this mechanism does not appear promising, given the uncertainties about the long-term efficacy of this level of O<sub>3</sub> depletion which is a strongest-case

scenario.

In future work, we plan to investigate the potential for climate change due to enhanced cloud cover and the direct biological effects of cosmic-ray secondaries at ground level.

## 5. Acknowledgments

We thank Tanguy Pierog for assistance in our local implementation of CORSIKA. AK is grateful for the financial support of the Honors Program at the University of Kansas, and for his research award from Vanderbilt University for this work, BT acknowledges a Small Research Grant from Washburn University.

Deleted: .

## 6. References

Aguirre, J., and R. Riding (2005), Dasycladalean Algal Biodiversity Compared with Global Variations in Temperature and Sea Level over the Past 350 Myr, *Palaios*, 20, 581-588

Alpen, E.L. (1998), *Radiation Biophysics* (San Diego: Academic Press)

Bancroft, B., N.J. Baker, and A.R. Blaustein (2007), Effects of UVB radiation on marine and freshwater organisms: a synthesis through meta-analysis, *Ecology Lett.* 10, 332-345

Binney, J. J. (2006), Triangulating the Galaxy, *Science* 311, 44-45



Björn, L.O., and R.L. McKenzie (2007), Attempts to Probe the Ozone Layer and the Ultraviolet-B Levels of the Past, *Ambio*, 36, 366-371

Blaustein, A. et al. (1998) Effects of ultraviolet radiation on amphibians: Field experiments, *Amer. Zool.* 38, 799-812

Cornette, J.L. (2007), Gauss-Vaniček and Fourier Transform Spectral Analyses of Marine Diversity, *Comput. Sci. Engineer.* 9, 62 doi: 10.1109/MCSE.2007.76

Davidson, A.T. (1998) The impact of UVB radiation on marine plankton, *Mutation Research/Fundamental and Molecular Mechanisms of Mutagenesis*, 422, 119-129  
doi:10.1016/S0027-5107(98)00183-3

Djemil, T., R. Attallah, and J.N. Capdevielle (2005), Simulation Of The Atmospheric Muon Flux With Corsika, *Int. J. Modern Physics A*, 20, 6950-6952

Ejzak, L.M. et al. (2007), Terrestrial consequences of spectral and temporal variability in ionizing photon events, *Astrophys. J.*, 654, 373-384

Foukal, P. et al. (2006), Variations in solar luminosity and their effect on the Earth's climate, *Nature*, 443, 161-166 doi:10.1038/nature05072

Formatted: Font: Italic

Gehrels, N. et al. (2003) Ozone Depletion from Nearby Supernovae, *Astrophys. J.*, 585, 1169-1176, doi: 10.1086/346127

Gies, D.R., and J.W. Helsel (2005), Ice Age Epochs and the Sun's Path through the Galaxy, *Astrophys. J.*, 626, 844-848

Häder, D. et al. (2003), Aquatic ecosystems: Effects of solar ultraviolet radiation and interactions with other climatic change factors, *Photochem. Photobiol. Sci.*, 2, 39-50

Harfoot, M.B.J. et al. (2007), A 2D atmospheric chemistry modeling investigation of Earth's Phanerozoic O<sub>3</sub> and near-surface ultraviolet radiation history, *J. Geophys. Res.*, 112, D07308

Hatch, A.C., and A.R. Blaustein (2000) Combined effects of UV-B, nitrate, and low pH reduce the survival and activity level of larval Cascades Frogs (*Rana cascadae*), *Arch. Environ. Contam. Toxicol.* 39: 494-499

Jagger, J. (1985), *Solar-UV Actions on Living Cells* (New York: Praeger)

Juckett, D.A. (2007), Correlation of a 140-year global time signature in cancer mortality birth cohorts with galactic cosmic ray variation, *Int. J. Astrobiology*, 6, 307-319

Kiesecker, J.M. et al. (2001) Complex causes of amphibian population declines. *Nature* 410, 681-683.

Formatted: Font: Italic

Krejci, A.J., A.L. Melott, and B.C. Thomas (2008), A Code To Compute High Energy Cosmic Ray Effects On Terrestrial Atmospheric Chemistry, *Astroparticle Physics*, submitted; arXiv:0804.3207.

Lieberman, B.S., and A.L. Melott (2007), Considering the Case for Biodiversity Cycles: Reexamining the Evidence for Periodicity in the Fossil Record, *PLoS One*, 2(8): e759  
doi:10.1371/journal.pone.0000759

Lockwood, M., and C. Fröhlich (2007), Recent oppositely directed trends in solar climate forcings and the global mean surface air temperature, *Proc. R. Soc. A*  
doi:10.1098/rspa.2007.1880

Madronich, S. (1993) UV radiation in the natural and perturbed atmosphere, in *UV-B Radiation and Ozone Depletion* (M. Tevini, Ed.) Lewis Publishers, Boca Raton, p. 35

McCallum, M. L. (2007) Amphibian Decline or Extinction? Current Declines Dwarf Background Extinction Rate, *Journal of Herpetology*. 41(3):483–491

Medvedev, M., and A.L. Melott (2007) Do extragalactic cosmic rays induce cycles in fossil diversity?, *Astrophys. J.*, 664, 879-889

Melott, A.L., B.C. Thomas, D.P. Hogan, L.M. Ejzak, and C.H. Jackman (2005) Climatic and Biogeochemical Effects of a Galactic Gamma-Ray Burst, *Geophys. Res. Lett.* 32, L14808

Melott, A.L. (2008) preprint submitted for publication. [arXiv:0807.4729](https://arxiv.org/abs/0807.4729)

Natarajan, L.C., A.L. Melott, B.M. Rothschild, and L.D. Martin (2007), Bone Cancer Rates in Dinosaurs Compared with Modern Vertebrates, *Trans. KS. Acad. Sci.*, 110, 155-158 (arXiv:0704.1912)

Pukkala, Eero et al. (1995), Incidence of cancer among Finnish airline cabin attendants, 1967-92, *Brit. Med. J.* 311, 649-652

Rohde, R., and R.A. Muller (2005) Cycles in Fossil Diversity, *Nature* 434, 208-210

Ruderman, M.A. (1974) Possible Consequences of Nearby Supernova Explosions for Atmospheric Ozone and Terrestrial Life, *Science*, 184, 1079-1081

Solanki, S.K. and N.A. Krivova (2003) Can solar variability explain global warming since 1970? *J. Geophys. Res.* 108, 1200 doi: 10.1029/2002JA009753

Scherer, K. et al. (2007), Interstellar-Terrestrial Relations: Variable Cosmic Environments, The Dynamic Heliosphere, and Their Imprints on Terrestrial Archives and Climate, *Space Science Reviews* 127, 327. Doi: 10.1007/s11214-006-9126-6

Shaffer, J.A. and R.S. Cervený (2004), Long-term ((250,000 BP to 50,000 BP) variations in ultraviolet and visible radiation (0.175-0.690 µm), *Global Planet. Change* 41, 111-120

Svensmark, H. (2006), Imprint of Galactic dynamics on Earth's climate, *Astronomische Nachrichten* 327, 866=870

Tevini, M. (1993) Effects of enhanced UV-B radiation on terrestrial plants, in *UV-B Radiation and Ozone Depletion* (M. Tevini, Ed.) Lewis Publishers, Boca Raton, p. 125-151

Thomas, B.C. et al. (2005), Gamma-Ray Bursts and the Earth: Exploration of Atmospheric, Biological, Climatic, and Biogeochemical Effects, *Astrophys. J.* 634, 509-533

Deleted: ¶

Thomas, B.C., C.H. Jackman, and A.L. Melott (2007), Modeling atmospheric effects of the September 1859 solar flare, *Geophys. Research Lett.* 34, L06810. doi: 10.1029/2006GL029174

Deleted: ¶

[Thomas, B.C., and M.D. Honeyman \(2008\). Amphibian nitrate stress as an additional terrestrial threat from astrophysical ionizing radiation events? \*Astrobiology\* 8\(4\): 731-733. doi:10.1089/ast.2007.0262](#)

Deleted: Thomas, B.C. and M.D. Honeyman (2008), Amphibian nitrate stress as an additional terrestrial threat from astrophysical ionizing radiation events? *Astrobiology*, submitted¶

Formatted: Font: Times New Roman

Formatted: Font: Times New Roman

Formatted: Font: Times New Roman

Formatted: Font: Times New Roman

## 7. Figure captions

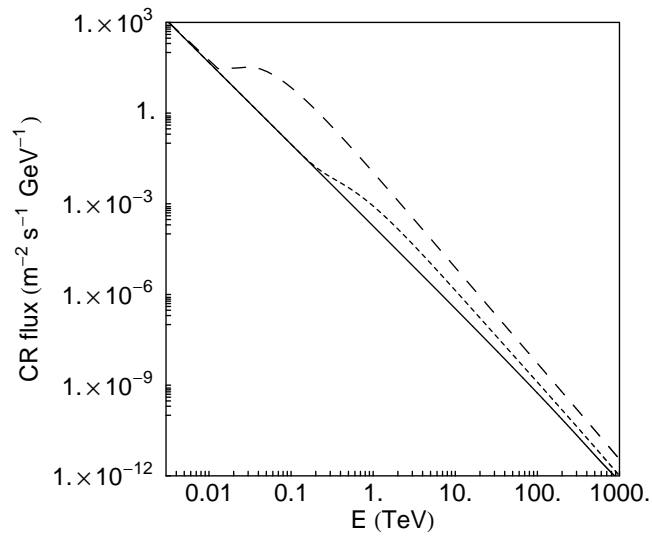


Figure 1: We show schematically the present cosmic ray flux spectrum at the Earth (solid line), and our minimum (short dash, called case 1) and maximum (long dash, called case 2) estimates of the spectrum enhanced due to reduced shielding from CRs produced at the galactic bow shock, when the solar system is at 70 pc north of the galactic disk. In this paper we assess atmospheric chemistry changes due to the two cases which bracket the reasonable range of intensity.

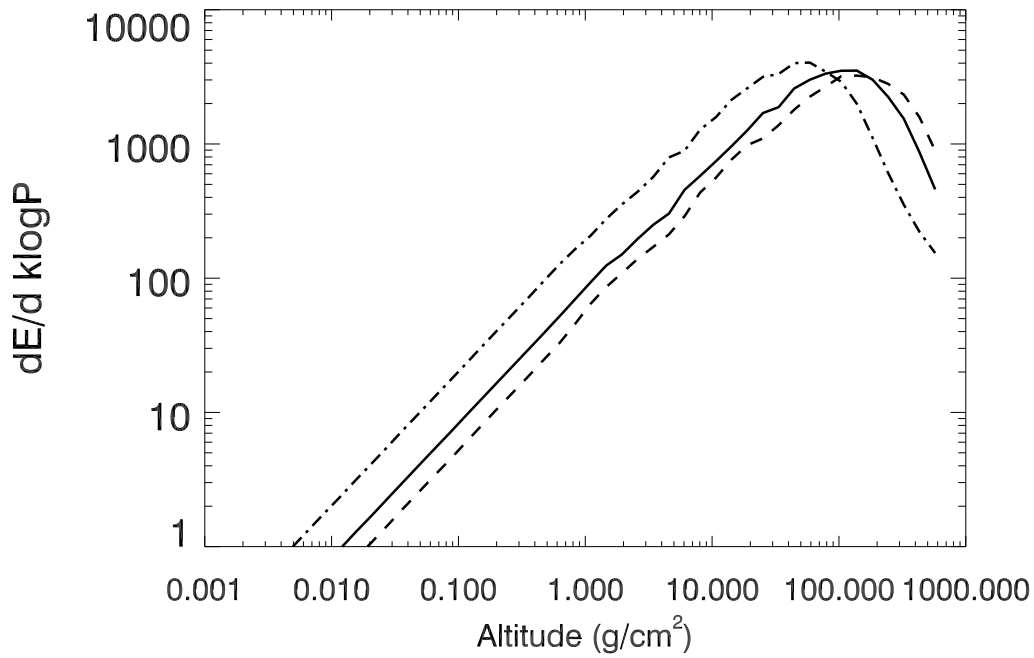


Figure 2a: We show the distribution of energy deposition in the atmosphere for ensemble of CORSIKA simulations for the cosmic ray spectrum with primaries between 10 GeV and 1 PeV, weighted as  $E^{-2.7}$  in analogy with the present observed spectrum at the Earth. This is plotted as fraction of the energy of the primary versus log of the column density (nearly linear with altitude) in bins of  $10 \text{ g/cm}^2$ . The zenith angle is  $0^\circ$  (vertical),  $45^\circ$ , and  $70^\circ$ , for dashed, solid, and dot-dash lines respectively.

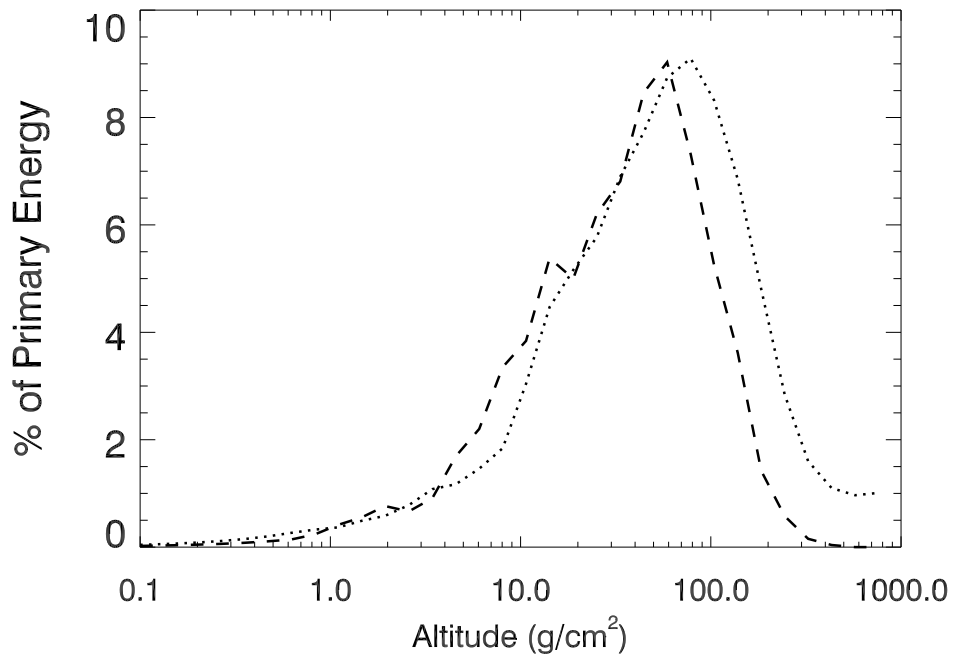


Figure 2b: Atmospheric energy deposition is plotted as percentage of primary energy, only for 70° zenith angle, for ensembles of 10 GeV and 1 PeV primaries (dashed versus dotted lines). Deposition varies only weakly with incident energy.



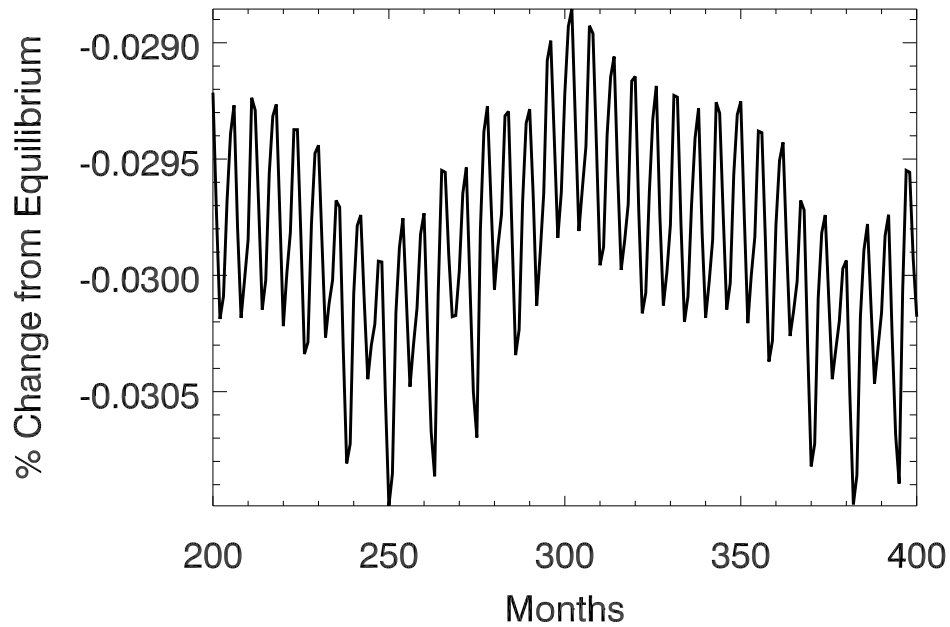


Figure 3a: Fractional changes in the atmospheric O<sub>3</sub> column density as a function of time after initial transients have stabilized, averaged on the entire surface of the Earth. Oscillations are due to annual and 11-year solar cycles. In this, Case 1, the changes are far too small to have any significant biological impact.

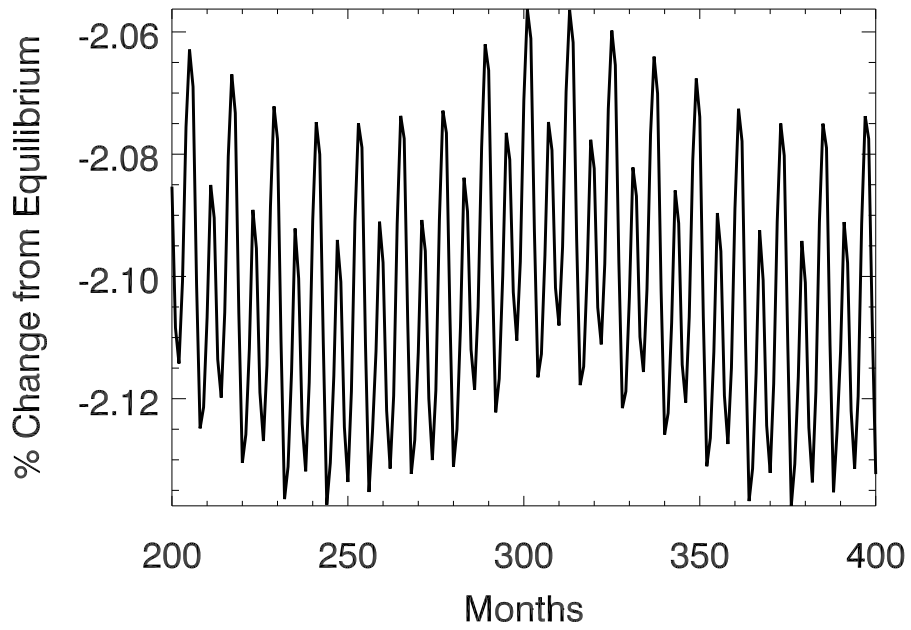


Figure 3b: As in Figure 3a, but for Case 2. Here, the size of the effect is not too different from present anthropogenic O<sub>3</sub> depletion, and so might have significant impact given the several My duration of the effect.

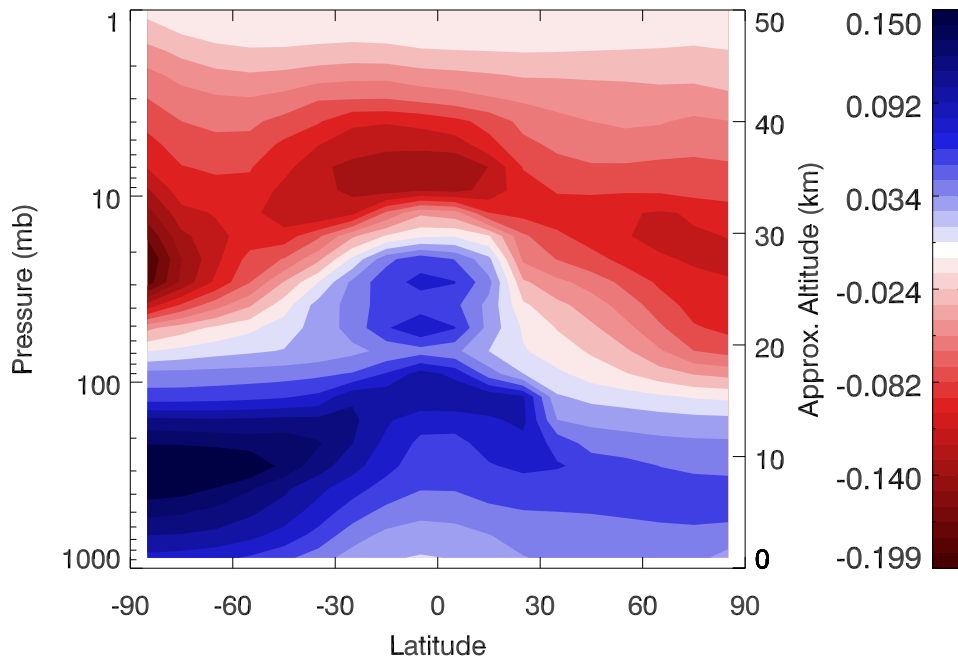


Figure 4a: A latitude, altitude plot of the percentage change in  $O_3$  volume number density in Case 1 due to the enhanced CR background. Note that stratospheric depletion is partially compensated by production at lower altitudes. The production comes both from CR as well as increased UVB leaking through the  $O_3$ -depleted upper atmosphere. Above the white layer is depletion, below is production.

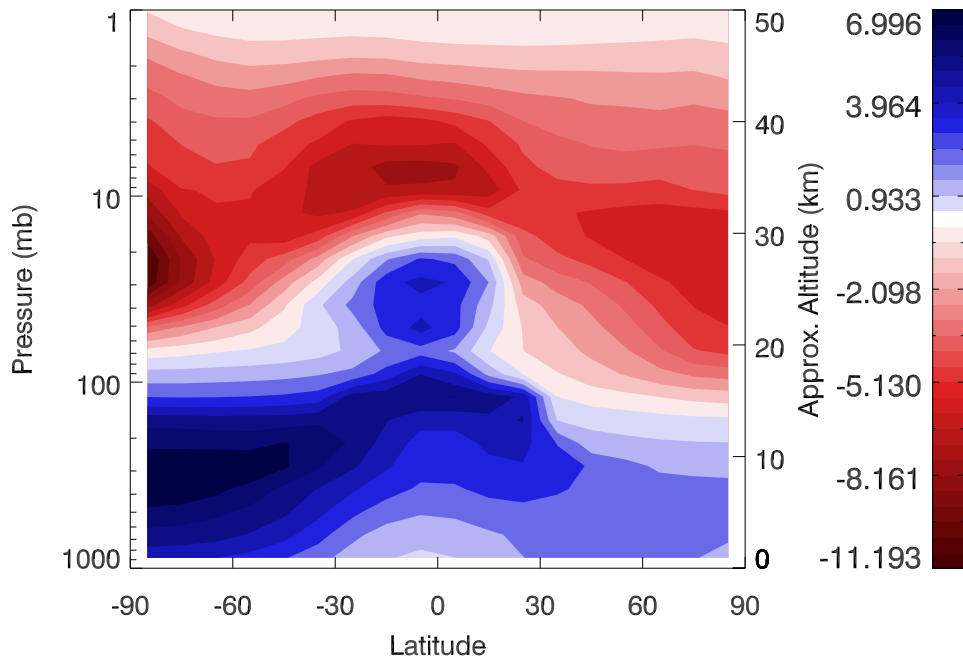


Figure 4b: As in Figure 4a, but for Case 2.

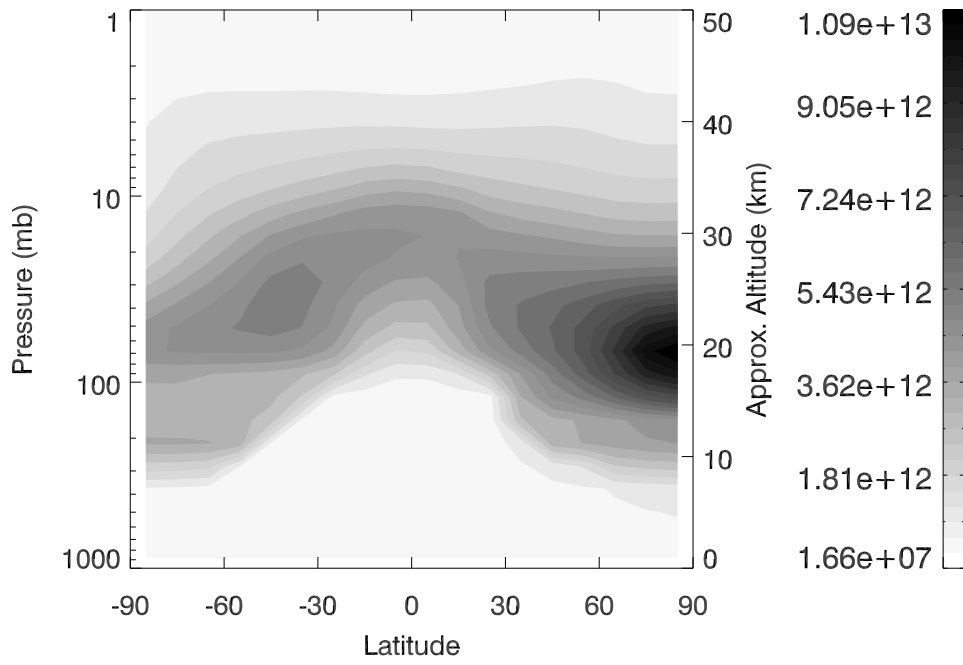


Figure 5: A latitude, altitude plot of the O<sub>3</sub> density in the unperturbed atmosphere.